Real-Time Deformation Measurement of Long-Span Bridge using Multi-Inertial Camera System

Ruizhe Chen [1,2,3,4], Wei Tu [1,2,3,4] , Qingquan Li [1,2,3,4], Zhipeng Chen [1,2,3,4], Bochen Zhang [1,2,3]

[1] Guangdong Key Laboratory of Urban Informatics, Shenzhen University, Shenzhen, Guangdong 518061, China;
- chenruizhe2021@email.szu.edu.cn, (tuwei, liqq, chenzp1990, zhangbc) @szu.edu.cn
[2] Ministry of Natural Resources Key Laboratory for Geo-Environmental Monitoring of Great Bay Area, Shenzhen University, Shenzhen, Guangdong 518061, China;
[3] Shenzhen Key Laboratory of Spatial Smart Sensing and Services, Shenzhen, Guangdong 518061, China;
[4] School of Architecture and Urban Planning, Shenzhen University, Shenzhen, Guangdong 518061, China;

Keywords: Inertial camera, Long-span bridge deformation, Multi-camera, Computer vision, Inertial measurement.

Abstract

Monitoring the deformation of long-span bridges is essential for assessing structural health and safety. The existing single-camera deformation measurement method is unable to meet the high-precision measurement requirement for the deformation of large-span bridges. This paper proposes a real-time deformation measurement method for the long-span bridge using multi-inertial camera system. The method is based on visual measurement which the target deformation is measured by multiple cameras. Meanwhile, inertial measurement is used to estimate the relative pose of the camera to compensate for camera motion errors. It is applied to the health monitoring system of a long-span bridge. The experimental results show that the method proposed in this paper is highly consistent with the hydrostatic leveling measurement, with a RMSE of 4.83mm. The method can accurately and real-time measure the deformation of large-span bridges with a promising engineering value.

1. Introduction

Bridges, as essential transportation infrastructures, ensure the connectivity of roads. Because of the combined influences of static load and moving load, the spatial shape of the bridge axis will continuously deform (Matsuoka et al., 2020). Excessive deformation risks structural damage which potentially results in severe accidents such as bridge collapse (Sun et al., 2018; Naser et al., 2018). Therefore, real-time measurement of the deformation is particularly important, as it can quickly assess the health and safety of bridges and assist relevant departments in inspection and maintenance (Feng et al., 2018).

A bridge with a single span greater than 100m is called a large-span bridge. The deformation of large-span bridges usually with the characteristics of large amplitude and dynamics deformation. Hence, this requires high-precision and real-time measurement for the long-span bridge. First of all, the total span length of large-span bridges usually is beyond 200m. The deformation will exceed 100mm when the moving load crosses the bridge. Therefore, the accuracy of the deformation measurement should meet the millimetre level or higher. What’s more, the bridge will deform multiple times within 1 second due to the impact of moving loads, which will require real-time measurement.

Traditional methods, such as robotic total stations and level stations, cannot well measure bridge deformation in a high-frequency manner (Santos et al., 2019). Single-camera measurement is commonly used for measuring the bridge deformation. It uses a camera to take photos of bridges. The measurement points are identified by extracting and matching features. Then, the pixel displacement of the points is calculated based on the time baseline parallax method. Finally, the pixel displacement will be converted into physical displacement to calculate the deformation of the bridge (Lee et al., 2020).

Though the single-camera method can achieve high-frequency deformation measurement at low cost (Yu et al., 2022), their uncertainty increases with distance, which means the farther the measurement distance, the poorer the accuracy. Some studies have overcome the limitation by collaborating with multi-cameras in unstable structures of bridges (Hu et al., 2023). Benchmarks are selected to compensate for the camera motion in the dynamic bridge. However, it is difficult to estimate the camera poses for the long-span bridges.

Inertial measurement is a new technology that utilizes sensors such as gyroscopes and accelerometers to measure the acceleration of the moving object in real-time to determine its position. Consequently, this paper proposes a multi-inertial camera system (MICS) for the deformation of large-span bridges by coupling computer vision with inertial sensors. Specifically, the multiple cameras in series are selected to measure high-frequency the deformation of targets in the long-span bridge. Meanwhile, inertial sensors are used to estimate the relative pose of the camera to compensate for camera motion errors. Ultimately, the deformation of the long-span bridge can be obtained by a mathematical model to achieve high-precision and real-time measurement.

The remainder of the paper is organized as following. The principle of a multi-inertial camera measurement system is first introduced in the Section 2, including the details of target identification, inertial measurement and the MICS model. Section 3 investigates on the proposed approach to measure deformation in a long-span bridge. The final section summarizes the method and outlook future research.

2. Methodology

2.1 Principle of MICS

For the long-span bridge, a multi-inertial camera system (MICS) is proposed for real-time deformation measurement, which can be flexibly arranged according to the field situation. The system mainly consists of multiple inertial cameras which can compensate for camera motion. As shown in Figure 1, the principle of the MICS has three steps as a blow.

First of all, multiple inertial cameras are installed along the bridge axis, and multiple measurement targets are placed between adjacent inertial cameras. Secondly, target images which are captured by the camera lens are extracted and tracked based on computer vision. Meanwhile, inertial sensors measure real-time camera poses which are vertical and pitch angle deformation. What’s more, the target position and camera pose are calculated by the MICS model to measure the deformation of the long-span bridge.

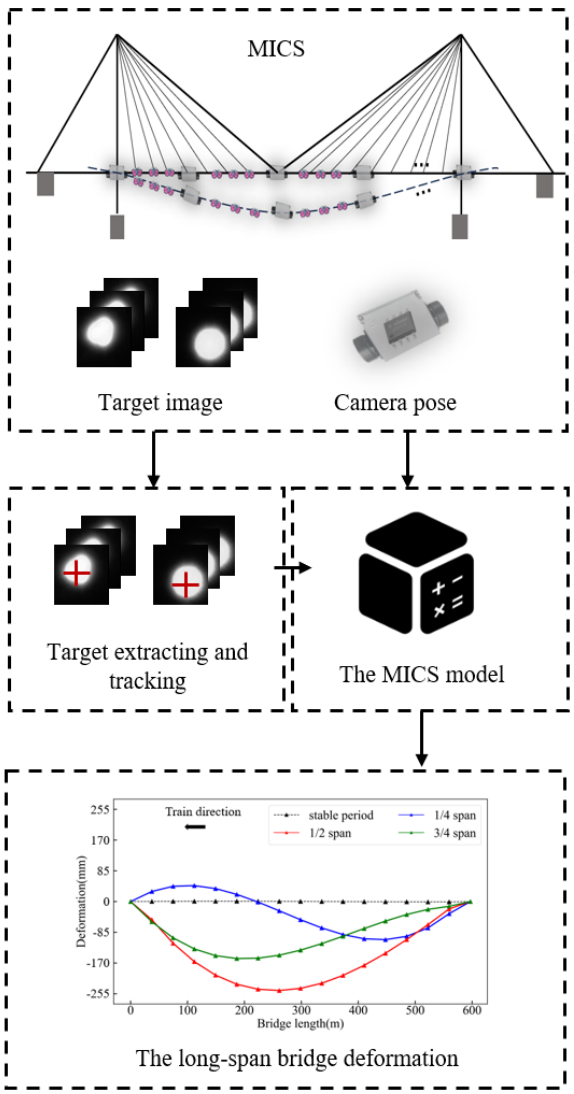

Figure 1 Multi-inertial camera system coupling computer vision with inertial sensors for deformation measurement of large-span bridge

The MICS is composed of multiple inertial cameras. One inertial camera integrates an inertial sensor and two cameras to simultaneously capture images and measure camera poses. The inertial camera is combined with high-frequency cameras mounted at both ends responsible for capturing targets. It is connected by a rigid body. The measurement frequency is set as 30Hz. Meanwhile, the relative pose of the camera is estimated by the high-precision inertial sensor inside the box.

2.2 Target Extracting and Tracking for the MICS

To overcome the effective measurement distance limitation of a single camera, multiple inertial cameras are collaboratively used for deformation measurement. Wherein some targets with infrared illumination are selected to improve extracting accuracy paired with inertial camera filters. After obtaining the image with the inertial camera, the coarse position of the target in the pixel plane is determined by a pre-calibrated region of interest (ROI) to reduce subsequent computational efforts. Here, the image quality in the ROI is enhanced based on the median filtering which can eliminate pixel abnormal values. In addition, the target pixels are calculated by the maximum weighted pixel value point position to identify the target centre. The principle is that the maximum value indicates that the position is the brightest area, which is usually located at the centre of the target's light emission which is relatively stable. The equation is as follows:

$$C = \mathrm{Max}\left[\sum_{u=1}^{8} \frac{h_v^u}{255} * h_v\right] \quad v = 1,2,3 \ldots z \tag{1}$$

where C = the vertical pixel coordinate of the point with the maximum weighted pixel value
v = the pixel point
h_v = the pixel value of v
h_v^u = the pixel value of each point in a 3 X 3 square area centred on v
u = the pixel number
z = the number of pixels in the area

The displacement of the pixel location to those of the stable period is calculated as the relative pixel deformation, as shown in the equation:

$$\Delta C = C_i - C_0 \tag{2}$$

where i = the sequential moment
0 = the stable period

2.3 Camera Motion Estimation based on Inertial Sensors

Most cameras are placed in bridge unstable structures and are prone to motion as shown in Figure 2. Therefore, an inertial camera is designed to compensate for the camera motion. When the bridge deforms, the position of the inertial camera changes accordingly. The deformation in pitch angle and vertical direction has the greatest impact on target imaging. Hence, the inertial sensors embedded inside the camera are used to measure them.

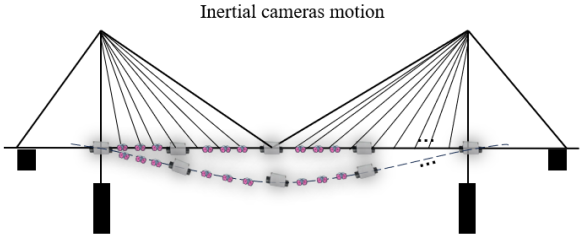

Figure 2 Camera motion when the bridge deforms

The inertial sensors can be divided into accelerometers and gyroscopes based on the different measurement objects. Specifically, the accelerometer is used to measure the vertical direction deformation of the camera which is the linear motion. The deformation in pitch angle is measured by the gyroscope. In the MICS, the accelerometers and gyroscopes are integrated into an inertial measurement unit to jointly measure the camera motion. What’s more, the main focus is on measuring camera motion relative to the most recent stable moment to avoid the long-term accumulation of inertial sensors’ errors.

In the camera motion estimation, the axis system of the inertial sensor and the axis system of the camera image space may not be parallel. Therefore, the conversion relationship between the camera pose deformation and the data measured by the inertial sensor is obtained in advance through calibration. And the camera vertical and pitch angle deformation data are corrected in inertial measurement based on the conversion relationship.

2.4 Camera Motion Compensation by the MICS Model

The MICS model is derived herein to compensate for camera motion to accurately measure the long-span bridge deformation in real time. The bridge mainly deforms in the vertical direction where the vertical and pitch angle deformation have the greatest impact on the measurement. Hence, the model can be established to compensate for the vertical direction and pitch angle deformation following the principle of geometric relationship for observing a single target with a single camera. Eventually, the models are combined based on mathematical relationships to derive herein the MICS model. Additionally, the target pixel displacement and camera vertical, pitch angle deformation are fed into the models which are solved by the least squares method to measure the long-span bridge deformation.

Assuming that the camera always remains stationary, as shown in Figure 3, the object point, image point, and optical center are collinear. In the figure, y is the physical deformation, and d is the pixel size, L is the horizontal distance from the camera to the target, f is the focal length.

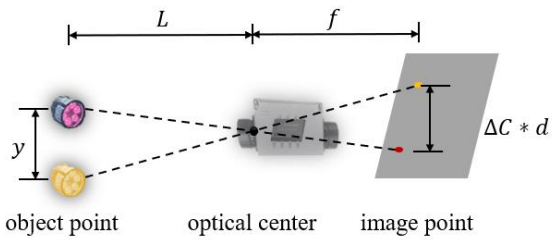

Figure 3 Camera imaging principle diagram

The target deformation can be calculated based on the camera imaging principle, as shown in the equation:

$$\frac{y}{\Delta C * d} = \frac{L}{f} = k \tag{3}$$

where k = the image scaling factor

However, as shown in Figure 4, when the bridge deforms, the deformation will be transmitted to the camera which is also installed on the bridge, resulting in deformation in the camera pose. Then the measurement errors will be made by deformation of the optical center. Therefore, some equations need to be constructed to correct the errors.

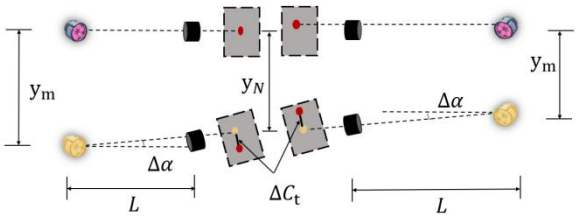

Figure 4 The deformation of the camera pose

This error is mainly caused by the deformation in the camera's vertical and pitch angle. The pixel deformation $\Delta \boldsymbol{C_e}$ caused by camera displacement of the target can be eliminated by the relative motion relationship based on the principle of geometric relationships, as shown in equation (4):

$$\Delta \boldsymbol{C_e} \cdot k = (\boldsymbol{y_m} - \boldsymbol{y_N}) \tag{4}$$

where $\boldsymbol{y_m}$ = the physical deformation variables of the target
$\boldsymbol{y_N}$ = the physical deformation variables of the camera

However, the image plane will rotate due to the deformation in camera pitch angle. Therefore, the $\Delta \boldsymbol{C_e}$ should be decomposed into the vertical direction of the rotated image plane, denoted as $\Delta \boldsymbol{C_d}$. From the geometric relationship, equation (5) can be obtained:

$$\Delta \boldsymbol{C_d} \cdot k = (\boldsymbol{y_m} - \boldsymbol{y_N}) \cdot \cos(\Delta \boldsymbol{\alpha_N}) \tag{5}$$

where $\Delta \boldsymbol{\alpha_N}$ = the deformation in camera pitch angle

When the camera pitch angle deforms, the stationary measurement target will also deform in the image plane. It can be found that this deformation has a non-linear relationship with the camera pitch angle change, as shown in equation (6):

$$\Delta \boldsymbol{C_\alpha} \cdot k = L \cdot sin(\Delta \boldsymbol{\alpha_B}) \tag{6}$$

Above all, the observation equation(7) of the inertial camera can be described by coupling the vertical displacement with the pitch angle deformation:

$$\Delta \boldsymbol{C_t} \cdot k = (y_m - y_N) \cdot \cos(\Delta \boldsymbol{\alpha_t}) \pm L \cdot \sin(\Delta \boldsymbol{\alpha_t}) \tag{7}$$

where ΔC_t = the vertical pixel displacement of the target at t

Equation (7) is the observation equation for a single inertial camera. The MICS model can be constructed by combining multiple inertial cameras.

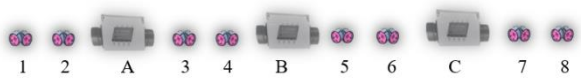

Figure 5 Schematic diagram of the MICS measurement

Taking Figure 5 as an example, there are three inertial cameras and eight targets. The MICS model is shown in equation (8). The equation can be solved by the least squares method.

$$\begin{cases} \Delta C_{At}^{1} \cdot k_{A1} = (y_1 - y_A) \cdot cos(\Delta\alpha_{At}) - L_{A1} \cdot sin(\Delta\alpha_{At}) \\ \Delta C_{At}^{2} \cdot k_{A2} = (y_2 - y_A) \cdot cos(\Delta\alpha_{At}) - L_{A2} \cdot sin(\Delta\alpha_{At}) \\ \Delta C_{At}^{3} \cdot k_{A3} = (y_3 - y_A) \cdot cos(\Delta\alpha_{At}) + L_{A3} \cdot sin(\Delta\alpha_{At}) \\ \Delta C_{At}^{4} \cdot k_{A4} = (y_4 - y_A) \cdot cos(\Delta\alpha_{At}) + L_{A4} \cdot sin(\Delta\alpha_{At}) \\ \Delta C_{Bt}^{3} \cdot k_{B3} = (y_3 - y_B) \cdot cos(\Delta\alpha_{Bt}) - L_{B3} \cdot sin(\Delta\alpha_{Bt}) \\ \Delta C_{Bt}^{4} \cdot k_{B4} = (y_4 - y_B) \cdot cos(\Delta\alpha_{Bt}) - L_{B4} \cdot sin(\Delta\alpha_{Bt}) \\ \Delta C_{Bt}^{5} \cdot k_{B5} = (y_5 - y_B) \cdot cos(\Delta\alpha_{Bt}) + L_{B5} \cdot sin(\Delta\alpha_{Bt}) \\ \Delta C_{Bt}^{6} \cdot k_{B6} = (y_6 - y_B) \cdot cos(\Delta\alpha_{Bt}) + L_{B6} \cdot sin(\Delta\alpha_{Bt}) \\ \Delta C_{Ct}^{5} \cdot k_{C5} = (y_5 - y_C) \cdot cos(\Delta\alpha_{Ct}) - L_{C5} \cdot sin(\Delta\alpha_{Ct}) \\ \Delta C_{Ct}^{6} \cdot k_{C6} = (y_6 - y_C) \cdot cos(\Delta\alpha_{Ct}) - L_{C6} \cdot sin(\Delta\alpha_{Ct}) \\ \Delta C_{Ct}^{7} \cdot k_{C7} = (y_7 - y_C) \cdot cos(\Delta\alpha_{Ct}) + L_{C7} \cdot sin(\Delta\alpha_{Ct}) \\ \Delta C_{Ct}^{8} \cdot k_{C8} = (y_8 - y_C) \cdot cos(\Delta\alpha_{Ct}) + L_{C8} \cdot sin(\Delta\alpha_{Ct}) \end{cases} \quad (8)$$

In summary, the deformation values of the inertial cameras and targets y_1, y_A,... can be solved by the least squares method to be treated as the deformation of measuring points in the long-span bridge. Then they will be fitted to obtain the overall deformation of the bridge, and finally achieve high-precision and real-time measurement of the deformation of a large-span bridge.

3. Experiment and Result Analysis

3.1 Laboratory Experimental Setup

The laboratory experiment in China is conducted to verify the accuracy and effectiveness of inertial camera compensation. The layout of the experiment is shown in Figure 6. The proposed inertial camera and two targets are employed at equal spacing in this experiment with a total length of 20m. Specifically, the camera is knocked by heavy objects to deform and the targets deform through an axis translation stage which can provide the true deformation.

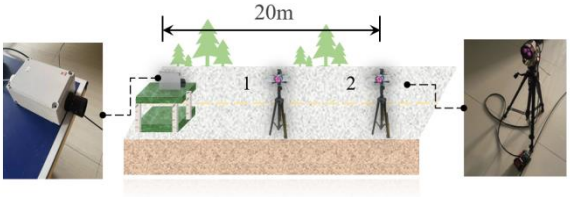

Figure 6 Layout of the laboratory experiment

3.2 Laboratory Experimental Results

The deformation of measurement targets 1 and 2 in the experiment during the knocking process is shown in the following Figure 7. From the figure, it can be displayed that the measurement results by the inertial camera are highly consistent with the truth. When the targets deform by 10mm, the root mean square errors(RMSE) of the inertial camera measurement results are 0.42mm and 0.44mm, respectively. In this experiment, it can be verified that the inertial camera is not affected by the camera's environment and effectively compensates for camera motion errors through the deformation model shown in equation (7).

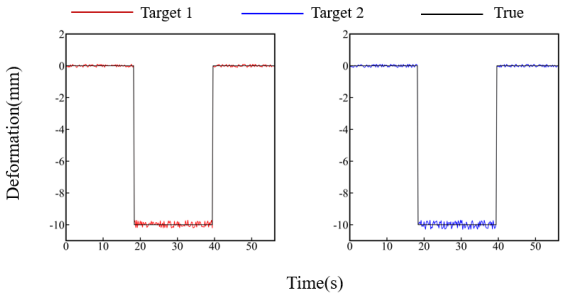

Figure 7 The target 1 and 2 deformation

3.3 Field Experimental Setup

The field experiment on the long-span bridge in China is conducted to verify the potential of the proposed MICS. The bridge crosses the waterway, which is a mixed cable-stayed double-track railway bridge with a total length of 1117.5m. The field experiment is mainly located in the cross-waterway main span of the bridge. Figure 8 shows the layout of the MICS. The site spans 600 meters and is equipped with 5 inertial cameras evenly spaced, with 3 targets placed between two cameras through the steel frame. The A and E cameras in the bridge pier are considered stable points without camera displacement. At the same time, the hydrostatic leveling is installed on the bridge, with a collection frequency of 1Hz, for comparison with the results measured by the MICS in this paper.

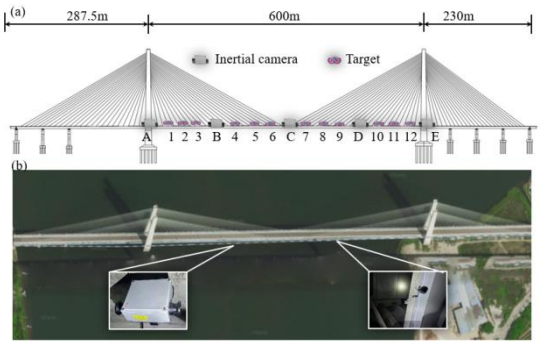

Figure 8 Layout of the MICS in Field experiment: (a) Measurement scheme; (b) Site overview of the bridge

When a train crosses through the bridge, it causes the inertial camera located at the main beam to move. The following Figures 9 and 10 show the vertical direction and pitch angle deformation of the camera caused by a certain train crossing the bridge. From the figure, it can be seen that the maximum deformation is beyond –250 mm and 0.08° respectively, resulting in measurement errors of up to 100mm or more. Therefore, it is essential to use the MICS model to compensate for the errors.

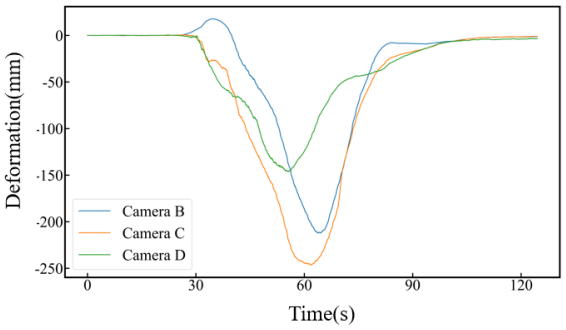

Figure 9 the vertical direction deformation of the camera

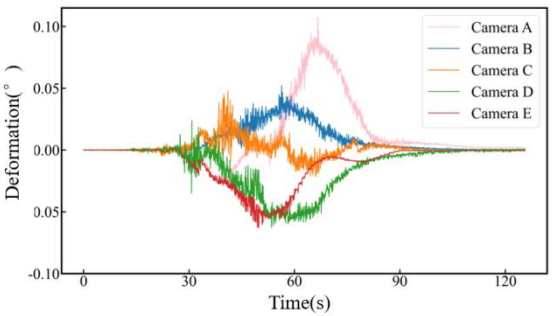

Figure 10 the pitch angle deformation of the camera

3.4 Field Experimental Results

The deformation of four measurement points in the middle of the main span of the bridge before and after a train crossing the bridge is shown in the following Figures 11, 12. When the train passes through the measurement points, the bridge deck is subjected to the pressure of moving loads, resulting in significant deformation of the bridge. The deformation is manifested as a trend of first upward deflection and then downward deflection. The trend of deformation is caused by the train's progress. Specifically, the train gradually approaches the measurement points, and there is a local upward wave peak deformation under the action of the load. When the train crosses through the points, the deformation of the bridge reaches its maximum with a wave valley situation. The accuracy, with the root mean square error (RMSE) of 4.76mm, is verified by comparing the MICS measurement results of bridge deformation with those of the hydrostatic leveling regarded as true.

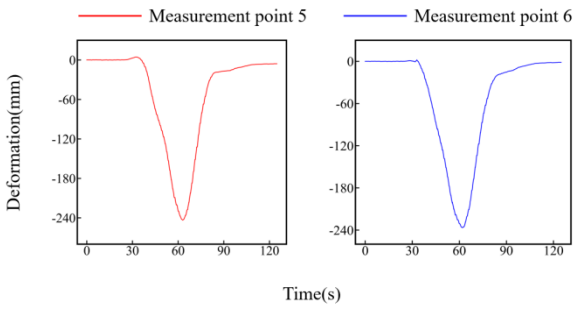

Figure 11 The measurement points 5 and 6 deformation

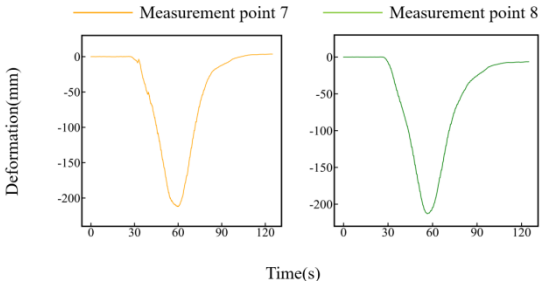

Figure 12 The measurement points 7 and 8 deformation

Figure 13 shows the overall deformation process of the bridge with a train passing. Following the direction of the train movement, the bridge will gradually deform. Specifically, when the train reaches 1/4 span, the force generated by the train is mainly concentrated here in camera B, thus the bridge reaches the maximum downward deformation at the place 450 meters. The left half of the bridge deforms to up due to uneven force distribution. When the train reaches 1/2 span, the maximum deformation, approximately 251.49mm, occurs near camera C at the place of 300 meters. When the train tail reaches a 3/4 span, the force generated by the train is mainly concentrated in camera D, where there is maximum deformation at the place of 150 meters. When the train has left, the bridge gradually recovers to a stable state.

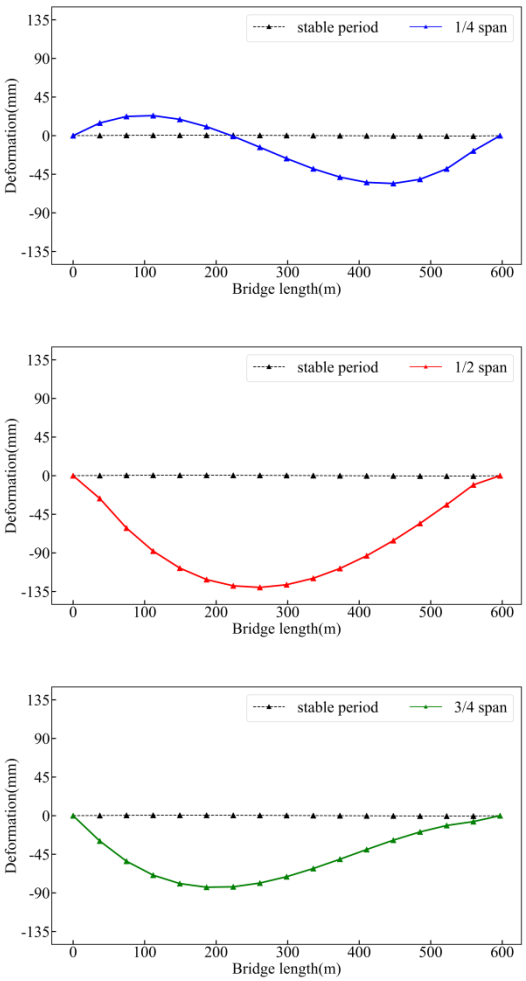

Figure 13 Measured deformation of the bridge under moving load

Furthermore, the RMSE of the MICS is 4.94mm compared to the hydrostatic leveling as true, which demonstrates the good performance of the proposed the MICS in practical engineering applications. The difference mainly occurs at measurement points with huge deformation of the large-span bridge due to different principles. Specifically, the principle of hydrostatic leveling measurement is connected pipes for measurement, which have a certain lag. However, the sampling time of the inertial camera can reach a millisecond level. Consequently, there is a difference between the measurement results of the MICS and the hydrostatic leveling in specific numerical values.

4. Conclusions

Monitoring the long-span bridge deformation is essential for assessing structural health and safety. This study presents a multi-inertial camera system to measure real-time deformation by fusing the computer vision and inertial sensors. It involves connecting multiple inertial cameras in series to extend the distance of precise visual measurement. Meanwhile, it addresses the camera motion problem due to the camera vertical displacement and pitch angle changing in multiple cameras measurement. Specifically, the MICS model couples the target deformation with the relative pose of the camera which is measured by inertial sensors to compensate for camera motion errors.

The results of the field experiment demonstrate the effectiveness of the proposed MICS approach with the RMSE of 4.94mm. The proposed MICS greatly enhances the stability of vision measurement in engineering applications, and can well meet the accuracy requirements of the long-span bridge deformation measurement. In the future, sensor technology innovation or algorithm improvement can be used to overcome the limitations of visual measurement that cannot be accurately measured in harsh environments.

Acknowledgements

We are grateful for the financial support from the Open Foundation of Technology Innovation Center of Smart City Spatiotemporal Information and Equipment Engineering of China Ministry of Natural Resources (grant numbers STIEIC-KF202307).

References

Matsuoka K, Kaito K, Sogabe M., 2020: Bayesian time–frequency analysis of the vehicle–bridge dynamic interaction effect on simple-supported resonant railway bridges. *Mechanical Systems and Signal Processing*, 135: 106373. doi:10.1016/j.ymssp.2019.106373.

Sun, L., Shang, Z., Xia, Y., Bhowmick, S., & Nagarajaiah, S. (2020): Review of bridge structural health monitoring aided by big data and artificial intelligence: From condition assessment to damage detection. *Journal of Structural Engineering*, 146(5), 04020073. doi: /10.1061/(ASCE)ST.1943-541X.0002535.

Naser M Z, Kodur V K R. Cognitive infrastructure-a modern concept for resilient performance under extreme events[J]. *Automation in Construction*, 2018, 90: 253-264. doi: 10.1016/j.autcon.2018.03.004.

Feng D, Feng M Q., 2018: Computer vision for SHM of civil infrastructure: From dynamic response measurement to damage detection–A review. *Engineering Structures*, 156: 105-117. doi: 10.1016/j.engstruct.2017.11.018.

dos Santos, R. C., Larocca, A. P. C., de Araújo Neto, J. O., Barbosa, A. C. B., & Oliveira, J. V. M., 2019: Detection of a curved bridge deck vibration using robotic total stations for structural health monitoring. *Journal of Civil Structural Health Monitoring*, 9, 63-76. doi: 10.1007/s13349-019-00322-1.

Lee J, Lee K C, Jeong S, et al. Long-term displacement measurement of full-scale bridges using camera ego-motion compensation[J]. *Mechanical Systems and Signal Processing*, 2020, 140: 106651. doi: 10.1016/j.ymssp.2020.106651.

Yu S, Su Z, Zhang J., 2022: Robust optical displacement measurement of bridge structures in complex environments. *ISPRS Journal of Photogrammetry and Remote Sensing*, 192: 395-408. doi: 10.1016/j.isprsjprs.2022.08.007.

Hu, B., Chen, W., Zhang, Y., Yin, Y., Yu, Q., Liu, X., & Ding, X., 2023: Vision-based multi-point real-time monitoring of dynamic displacement of large-span cable-stayed bridges. *Mechanical Systems and Signal Processing*, 204, 110790. doi: 10.1016/j.ymssp.2023.110790.